Water Air Soil Pollut (2020) 231: 254
https://doi.org/10.1007/s11270-020-04547-5

Degradation of a Sunset Yellow and Tartrazine Dye Mixture: Optimization Using Statistical Design and Empirical Mathematical Modeling

G. E. do Nascimento · V. O. M. Cavalcanti · R. M. R. Santana · D. C. S. Sales · J. M. Rodríguez-Díaz · D. C. Napoleão · M. M. M. B. Duarte

Received: 11 December 2019 / Accepted: 23 March 2020 / Published online: 16 May 2020

Abstract The food industry is considered to be one of the greatest sources of environmental contamination produced by dyes. Moreover, a large number of commercial food dyes and their by-products have been shown to be toxic, having chronic effects on human health. The search for efficient processes with which to treat these compounds is, therefore, necessary. In this work, the photo-peroxidation and photo-Fenton processes using UV-C and sunlight radiations were evaluated in order to degrade two synthetic dyes commonly found in food industry wastewater, sunset yellow and tartrazine, in an aqueous mixture. The preliminary results showed that the photo-Fenton/UV-C system was the most efficient. The ANOVA analysis results indicated a good fit of the model. The higher degradations were obtained using 50 mg L^{-1} of [H_2O_2], 1 mg L^{-1} of [Fe], a pH of 3.5, and a lower surface area/volume ratio (0.02 cm^2 mL^{-1}). In the kinetic study, a good fit was found for the kinetic model proposed by Chan and Chu. Degradations higher than 99% and 78% were obtained for the chromophore and aromatic groups, respectively, in 180 min. Toxicity tests showed that post-treatment samples did not interfere in the development of *Lactuca sativa* seeds and *Escherichia coli* and *Salmonella enteritidis* bacteria strains. The ph(Basu and Kumar 2015), since this parameter is often associated with the quality of the final product (Wang et al. 2014). Food colorings are classified according to how they are obtained and can be natural, artificial, or synthetic (Rovina et al. 2016). The use of synthetic dyes is considered to be more advantageous owing to their higher stability, brighter color, and lower price when compared with natural dyes (Carocho et al. 2014).

The synthetic dyes most frequently used in the food industry are azo dyes (-N = N-). Of these, the most common are the tartrazine and sunset yellow anionic dyes (Peláez-Cid et al. 2016; Lipskikh et al. 2018), which are used to color jellies, ice creams, soft drinks, and alcoholic drinks, among others. Despite their extensive use, several studies have identified the chronic effects that food dyes have on human health (Chung 2016; Okafor et al. 2016; Elbanna et al. 2017).

G. E. do Nascimento (✉) · V. O. M. Cavalcanti · R. M. R. Santana · D. C. Napoleão · M. M. M. B. Duarte
Departamento de Engenharia Química, Universidade Federal de Pernambuco, Av. Prof. Arthur de Sá, s/n, Recife, PE 50740-521, Brazil
e-mail: grazielen@yahoo.com.br

D. C. S. Sales
Escola Politécnica de Pernambuco, Universidade de Pernambuco, Rua Benfica, 455, Madalena, Recife, PE 50720-001, Brazil

J. M. Rodríguez-Díaz
Laboratorio de Análisis Químicos y Biotecnológicos, Instituto de Investigación, Universidad Técnica de Manabí, Portoviejo, Ecuador

J. M. Rodríguez-Díaz
Departamento de Procesos Químicos, Facultad de Ciencias Matemáticas, Físicas y Químicas, Universidad Técnica de Manabí, Portoviejo, Ecuador

J. M. Rodríguez-Díaz
Programa de Pós-graduação em Engenharia Química, Universidade Federal da Paraíba, João Pessoa 58051-900, Brazil

Many studies published in the last few decades have reported the dangers of tartrazine dye, identifying its potentially deleterious effects, such as food allergies, mutagenicity, carcinogenicity, and phototoxicity (Gupta et al. 2011; Soares et al. 2015; Khayyat et al. 2017). An excessive consumption of sunset yellow dye can cause changes, such as attention deficit hyperactivity disorder (ADHD) in children, in addition to cancer, asthma, immunosuppression, eczema, migraines, and anxiety (Rovina et al. 2016).

Moreover, the presence of coloring substances in water bodies has a negative effect on the environment, which is associated with the fact that they reduce light penetration and dissolved oxygen levels (Chekira et al. 2017). The negative impacts of synthetic food dyes on living organisms and the environment signify that it is necessary to use efficient methods to treat wastewater before its release into the receiving bodies (Tikhomirova et al. 2018).

In this respect, advanced oxidative processes (AOP) can be applied to promote the degradation of a variety of organic compounds, including dyes (Almeida et al. 2019). These treatments have been shown to be efficient, since they are based on the oxidation power of hydroxyl radicals, which can be supplied by applying electrical energy, radiation, chemicals, or a mixture of these methods (Wang and Xu 2012; Banaschik et al. 2018). One of these processes is the UV/H_2O_2 or photoperoxidation action, which involves the photolysis of H_2O_2 in order to generate the hydroxyl radicals. The Fenton reaction occurs owing to the combined action of ferrous ion and H_2O_2, which generates hydroxyl radicals. In the photo-Fenton process, these radicals result from the association of the Fenton reaction with a light source (Cetinkaya et al. 2018).

The photo-Fenton process has been applied as a pretreatment to improve biodegradability and is also a means of propitiating the mineralization of persistent pollutants, whose eventual products are water, CO_2, and inorganic salts (Oller et al. 2011; Vedrenne et al. 2012). However, sometimes only partial mineralization is achieved, making it essential to ensure that the products formed are not toxic (Nagel-Hassemer et al. 2011; Rizzo 2011). Santos et al. (2018) evaluated the toxicity of a mixture of erythrosine and bright blue food dyes before and after AOP using *Lactuca sativa* seeds, and found a reduction in the toxic potential of the solution after treatment.

During the use of AOP, it is necessary to optimizate the operating conditions. In traditional optimization methods, only one parameter is varied at a time, without an evaluation of the interactions between the parameters that affect the process (Nair et al. 2014; Shojaeimehr et al. 2014). One alternative when simultaneously analyzing these variables is, therefore, the use of statistical tools, such as factorial design (Santiago et al. 2018). Gadekar and Ahammed (2019) used a central composite design to obtain the best working conditions and to evaluate the influence of three parameters on the removal of the blue 79 dispersive dye.

The objective of this work was, therefore, to study the degradation of a sunset yellow and tartrazine dye mixture, that is widely employed in the food industry by using advanced oxidative processes. The 2^4 factorial central composite design (CCD) was used to evaluate the effects of the variables on the percentage of degradation of the dye mixture in order to optimize the experimental conditions. A variance analysis (ANOVA) was subsequently performed in order to verify its fit to the regression model. The degradation kinetics of the compounds was evaluated. The toxicity before and after submission to the AOP using seeds and bacteria was also investigated, and the biodegradability was additionally analyzed.

1 Materials and Methods

1.1 Dyes and Reagents

The sunset yellow (SY) and tartrazine (T) food dyes were provided by the F. Trajano company. All reagents used in this study were of an analytical grade and had undergone no further purification. Hydrogen peroxide (H_2O_2, 30% v/v, Modern Chemistry, standardized) was used as an oxidizing agent, while the source of the iron was ferrous sulfate heptahydrate ($FeSO_4.7H_2O$, 99.98% purity, Vetec). The pH of the solutions was adjusted with 0.1 mol L^{-1} H_2SO_4 (97% purity, Merck) and with the aid of a pH meter (Quimis, Q400AS). All the solutions were prepared with distilled water.

1.2 Identification of Characteristic Wavelengths and Analytical Curves for Dye Quantification

An ultraviolet/visible spectrophotometer (Thermo Scientific brand, model Genesys 10S) with a

spectral scanning range of 190 to 1100 nm was used to determine the wavelengths (λ) characteristic of the SY and T dyes. A scanning analysis of the initial solutions in the pH used in this work (2 to 6) was also performed. Analytical curves (for each of the λ selected), with a concentration range of 1 to 10 mg L^{-1}, were used: correlation coefficients (r) greater than 0.99; values of LD < 0.09 mg L^{-1}, LQ < 0.33 mg L^{-1}, and CV < 2.75%.

1.3 Preliminary Evaluation of the Degradation of the Dye Mixture

In order to identify the most efficient advanced oxidative process (AOP) as regards the degradation of the SY and T dye mixtures, the photo-peroxidation and photo-Fenton processes were tested using UV-C and sunlight photochemical reactors. The reactor with UV-C radiation was composed of three lamps (Philips), arranged in parallel, with a total power of 90 W and an emission of photons of 1.89×10^{-3} W cm^{-2}. The reactor with sunlight radiation (artificial solar) used a lamp (Osram) with a power of 300 W and an emission of photons of 12.54 W cm^{-2} in the visible band, 7.4×10^{-2} W cm^{-2} in the range of UV-A/UV-B, and 9.4×10^{-4} W cm^{-2} in the UV-C range.

The assays were performed under the following conditions: an iron concentration ([Fe]) of 1 mg L^{-1}, a hydrogen peroxide concentration ($[H_2O_2]$) of 50 mg L^{-1}, with the pH equal to 5.5 (natural pH of the solution), and 1-h exposure to radiation. The experiments were carried out at 28 ± 1 °C and at an atmospheric pressure of 1 atm, using 100-mL beakers, to which 50 mL of the mixture containing 10 mg L^{-1} of each dye was added.

1.4 Model Employed to Predict the Degradation of the Dye Mixture and a Study of the Influence of Process Variables Using a Statistical Design

The optimization of the operational conditions was performed for the AOP system selected in the aforementioned study. The 2^4 factorial central composite design (CCD) with a center point was carried out with the objective of evaluating the effects of the following variables: concentration of hydrogen peroxide ($[H_2O_2]$), concentration of iron ([Fe]), pH, and time as regards the percentage of degradation of the SY and T dye mixture. The levels evaluated were the following: $[H_2O_2]$ (50, 100, and 150 mg L^{-1}), [Fe] (1, 3, and 5 mg L^{-1}), pH (3.5, 4.5, and 5.5), and time (30, 60, and 90 min). The tests were performed in a random order and the central point in triplicate, with a total of 19 experiments. The experiments were conducted at 28 ± 1 °C and at an atmospheric pressure of 1 atm in 60 min, using 50 mL of dye mixture. The variables and exposure times were defined on the basis of previous studies.

The response used to evaluate the efficiency of the process employed was the percentage of degradation of dye mixture. The second-order polynomial equation (Montgomery 2008) was used to analyze the experimental results and is described in Eq. (1).

$$Y = \beta_0 + \sum_{i=1}^{n} \beta_i X_i + \sum_{i=1}^{n} \beta_{ii} X_i^2 + \sum \sum_{i<j=1}^{n} \beta_{ij} X_i Y_j \quad (1)$$

where Y is the predicted response (percentage of degradation), β_o is the displacement term, β_i is the linear effect, β_{ij} is the first-order interaction, β_{ii} is the quadratic effect, and X_i and X_j are the independent variables of the model.

A two-way analysis of variance (ANOVA) was applied to the response, considering both the linear and quadratic effects for the variables $[H_2O_2]$, [Fe], pH, and time, and was used to verify the fit to the second-order regression model. A multiple regression analysis was used to estimate the coefficients of the model for each of the λ studied. The adequacy of the model was evaluated by determining the coefficient of determination (R^2) and the pure error (MS pure error).

In addition, it was possible to observe the influence of the variables on the percentage of degradation for each of the λ studied from the response surfaces, which were generated using Statistica 10.0 software. Statistically significant effects were assessed at a confidence level of 95%.

1.5 Volume Ratio o/Volume Ratio of the Solution on Degradation Efficiency

In order to verify whether the ratio between the surface area (A_{sup}) and the volume of the solution (V_{sol}) had a significant influence on the degradation of the dye mixture, experiments were conducted at 28 ± 1 °C and at an atmospheric pressure of 1 atm under the conditions defined in the two previous studies and in the time of

60 min. The A_{sup}/V_{sol} ratios ($cm^2\ mL^{-1}$) evaluated were 0.02 (19.5/1000), 0.03 (13.0/500), 0.05 (9.0/200), 0.08 (7.5/100), and 0.11 (5.5/50).

1.6 Kinetic Evaluation of the Degradation of the Dye Mixture

The kinetic study of the degradation of the dye mixture was performed under the best conditions defined from the studies performed in the previous items at a temperature of 28 ± 1 °C and at an atmospheric pressure of 1 atm in the times of 10, 20, 30, 45, 60, 90, 120, 150, and 180 min.

The adjustment of the experimental data obtained for the kinetic model proposed by Chan and Chu (2003) and presented in Eq. (2) was then verified.

$$C = C_0\left(1-\frac{t}{\rho+\sigma t}\right) \tag{2}$$

where C is the concentration of the solution (mg L^{-1}) after a time t (min) and C_0 is the initial concentration of the solution (mg L^{-1}). The parameters ρ and σ represent the reaction kinetics (min) and the oxidation capacity of the system (dimensionless), respectively.

Upon deriving Eq. (2) with time, Eq. (3) was obtained.

$$\frac{dC/C_0}{dt} = \frac{-\rho}{(\rho+\sigma t)^2} \tag{3}$$

According to Chan and Chu (2003), when t is zero, the initial removal rate of the compound ($1/\rho$) (Eq. (4)) is obtained and the greater the $1/\rho$, the faster the compound decay rate. When t is long and approaches infinity, the maximum oxidation capacity ($1/\sigma$) of the process at the end of the reaction is obtained (Eq. (5)).

$$\frac{dC/C_0}{dt} = \frac{1}{\rho} \tag{4}$$

$$\frac{1}{\sigma} = 1-\frac{C_{t\to\infty}}{C_0} \tag{5}$$

An estimation of the dye conversion (degradation efficiency) was also performed on the basis of Eq. (6).

$$X = 100\left(1-\frac{C_f}{C_0}\right) \tag{6}$$

where X (%) is the conversion and C_f (mg L^{-1}) is the final concentration of the solution.

In addition, the samples collected at the times of 30, 60, 120, 150, and 180 min were monitored by using spectral scans in the range of 190 to 600 nm in order to verify the presence of peaks related to the formation of possible reaction intermediates.

The residual concentration of H_2O_2 was determined using a colorimetric semi-quantitative method with MQuant Test Strips (Merck), where $[H_2O_2]$ ranges from 0 to 25 mg L^{-1}. The measurement was performed at the end of the kinetic experiment (180 min).

1.7 Toxicity Study and Evaluation of Biodegradability

The toxicity tests were performed under the same conditions as those employed in the kinetic study, before and after the submission of the dye mixture to the previously selected AOP for 180 min. *Lactuca sativa* seeds, along with *Escherichia coli* UFPEDA 224 and *Salmonella enteritidis* UFPEDA 414 bacteria, were used.

The evaluation of toxicity using seeds consisted of exposing the *Lactuca sativa* seeds to the dye mixture before and after treatment. In the latter case, the following dilutions were employed: 100, 70, 50, 10, 5, and 1%. The analyses were performed in triplicate, according to the methodology described by Zaidan et al. (2017). The results of the relative growth index (RGI) and the germination index (GI) were evaluated according to Young et al. (2012).

The bacteriological toxicity experiments were carried out with strains of *Escherichia coli* and *Salmonella enteritidis* cultivated overnight in a Mueller Hinton agar medium (AMH) at 36 °C, according to the methodology described by Nascimento et al. (2018a). Trials were performed in triplicate with the dye mixtures before and after treatment, without dilution and at dilutions of 1:100 (10^{-2}) and 1:1000 (10^{-4}).

The evaluation of the biodegradability of the dye mixture was determined by analyzing the chemical oxygen demand (COD) and the biochemical oxygen demand (BOD), which allowed to calculate the COD/BOD ratio. The analyses were

performed with the samples before and after the degradation process in the time of 180 min, under the same conditions as those employed in the kinetic study. The COD was determined on the basis of the 5220D method and the BOD adapted from the 5210B method, both from the Standard Methods for the Examination of Water and Wastewater (Rice et al. 2012).

2 Results and Discussion

2.1 Identification of Characteristic Wavelengths

The absorption spectra of the SY and T dye solutions obtained by means of scanning allowed us to identify five characteristic wavelengths (λ). The results for the various pH analyzed are presented in Fig. 1.

The UV-visible absorption spectra (Fig. 1) had two major peaks in the visible region at λ of 428 and 482 nm, along with three peaks in the ultraviolet region, where λ was equal to 234, 258, and 314 nm. The major peaks in the visible region are responsible for the color and are attributed to the n-π* transition absorption of the chromophore groups of the dye molecule. It is, however, possible to attribute peaks of 234, 258, and 314 nm to the π-π* transition absorption, which is, according to Oancea and Meltzer (2013) and Ghoneim et al. (2011), related to the aromatic rings bound to dye molecules. The monitoring of these peaks is important because it is indicative of the breakage of the aromatic groups in the molecule of the dyes, and the consequent degradation of these compounds. As Fig. 1 shows, no displacement of the λ studied was found as a function of the initial pH of the solution.

2.2 Preliminary Evaluation of the Degradation of the Dye Mixture

The results obtained for the degradation of SY and T dyes when using the photo-peroxidation and photo-Fenton processes are presented in Table 1. It is worth mentioning that the most effective AOP was selected from these results.

Photo-peroxidation was less efficient as regards the degradation of the dye mixture than was the process using iron, i.e., the photo-Fenton process (Table 1). Similar results were obtained when comparing the use of UV-C and sunlight radiation in the photo-Fenton process. However, the choice of UV-C radiation was made for the subsequent studies, upon considering that the reactor used has a total power that is 3.33 times smaller than the sunlight reactor, thus reducing the costs of the process with respect to the amount of electrical energy needed for degradation.

2.3 Model Employed to Predict the Degradation of the Dye Mixture and Study the Influence of Process Variables Using a Statistical Design

The 2^4 factorial central composite design (CCD) with a central point in triplicate was used to evaluate the interaction between the four variables and the degradation of the dye mixture using a second-order polynomial equation. The variables studied were coded as follows: hydrogen peroxide concentration (X_1), iron concentration (X_2), pH (X_3), and time (X_4). The equations in the regression model for each of the λ studied were attained by employing the coefficients obtained in the effect estimation table obtained by using the Statistica 10.0 software and discarding the effects that were not statistically significant ($p \geq 0.05$) (Eqs. (7–11)). The positive and negative signals in the terms indicate the synergistic and antagonistic effect, respectively.

$$Y_{234\text{nm}} = 68.67 - 2.30X_1 - 13.23X_1X_1 - 19.27X_2 - 2.92X_3 + 7.22X_4 + 2.26X_2X_3 + 1.41X_3X_4 \quad (7)$$

$$Y_{258\text{nm}} = 76.77 - 1.05X_1 - 15.28X_1X_1 - 19.29X_2 - 9.54X_3 + 5.50X_4 + 3.79X_2X_3 + 0.55X_3X_4 \quad (8)$$

$$Y_{314\text{nm}} = 34.57 + 1.64X_1 - 32.61X_2 - 4.16X_3 + 1.59X_4 + 3.16X_2X_3 \quad (9)$$

$$Y_{428\text{nm}} = 92.00 + 1.31X_1 - 0.53X_1X_1 - 5.28X_2 - 7.26X_3 - 0.78X_4 + 0.92X_1X_2 + 0.96X_1X_3 - 5.14X_2X_3 - 0.37X_2X_4 - 0.61X_3X_4 \quad (10)$$

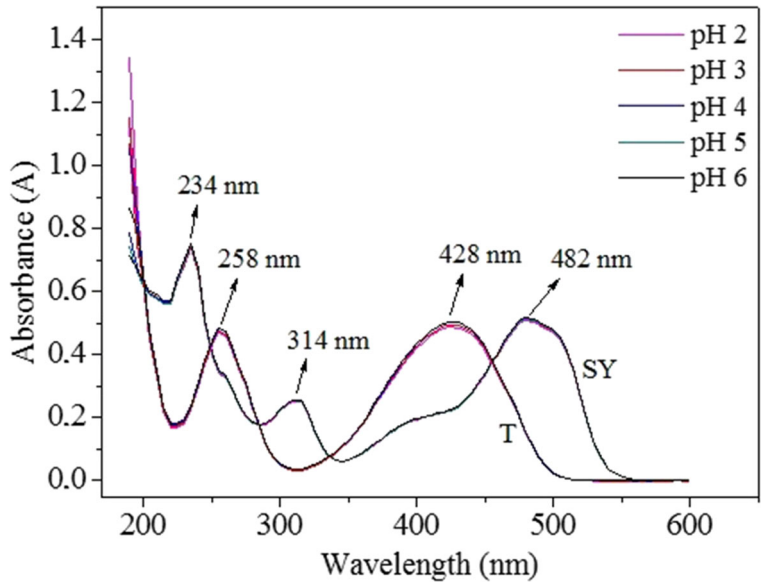

Fig. 1 UV-visible absorption spectra of SY and T dyes

$$Y_{428\text{nm}} = 93.93 + 0.47X_1 - 3.96X_2 - 4.96X_3 - 0.87X_4 + 0.66X_1X_2 + 0.72X_1X_3 + 0.62X_1X_4 - 3.68X_2X_3 - 0.46X_2X_4 - 0.42X_3X_4 \quad (11)$$

The estimates of the effects obtained by using a two-way ANOVA (linear and quadratic effects; pure error) for the degradation of the dye mixture at a confidence level of 95% are shown in Table 2. Note that the quadratic effects of the variables X_2, X_3, and X_4 refer to linear combinations of other effects and were not estimated for the λ studied. Moreover, according to the effect estimates, [Fe] had a greater influence on the degradation of the mixture of the colorants for the λ of 234, 258, and 314 nm. However, in the case of the λ of 428 and 482 nm, this influence was observed for the pH variable. This result is possibly owing to the fact that some chromophoric groups are influenced by the pH, and may even have a band shift as a function of the initial pH variation of the solution. With regard to the groups observed in λ that were equal to 234, 258, and 314 nm, aromaticity is present, which makes the degradation process more difficult, thus requiring the presence of a catalyst to increase the efficiency of the process.

Table 2 shows that all the main effects were statistically significant at a confidence level of 95% for all the λ studied, with the exception of the quadratic effect (X_1X_1) of [H_2O_2] for the λ of 314 and 482 nm. In the case of the λ of 234 and 258 nm, the statistically significant interaction effects were [Fe] vs pH (X_2X_3) and pH vs time (X_3X_4). However, for the λ of 314 nm, only the interaction effect [Fe] vs pH (X_2X_3) was significant. In the case of the λ of 428 and 482 nm, all interaction effects were significant except [H_2O_2] vs time (X_1X_4) for the λ of 428 nm.

Table 1 Percentages of degradation for each of the λ studied

Process	Radiation	% of degradation				
		234 nm	258 nm	314 nm	428 nm	482 nm
Photo-peroxidation	Sunlight	0.0	5.2	9.4	20.8	31.0
Photo-peroxidation	UV-C	48.9	62.6	55.3	86.1	90.5
Photo-Fenton	Sunlight	80.6	82.8	63.1	95.4	97.2
Photo-Fenton	UV-C	81.1	83.0	63.6	95.7	97.6

The results of the two-way ANOVA analysis indicated the good adequacy of the experimental data for the model, for each of the λ studied, with a coefficient of determination (R^2) ranging from 0.9781 to 0.9955 and low values of MS pure error (0.0110–0.1733). This can be confirmed by comparing the percentages of degradation obtained experimentally and those predicted by the models, as shown in Fig. 2.

As interaction effects between the variables were observed, response surfaces were generated by employing the Statistica 10.0 software, with the objective of carrying out a joint evaluation of the influence of the variables studied on the percentage of degradation, for each of the λ studied. Figures 3, 4 and 5 show the response surfaces of interaction effects [Fe] vs pH, pH vs time, [H_2O_2] vs pH, [H_2O_2] vs [Fe], and [Fe] vs time, respectively.

In the degradation evaluate (%), through the use of response surface graphs, it is possible to verify that the results obtained are arranged in two layers. The lower layer, in the darker part, has the condition in which there is the best combination of variables whose interaction effect was significant. The upper layer, on the other hand, has different curvatures, in which the maximum degradation is observed at the apex of that curve.

An analysis of Fig. 3 indicates that, for lower levels of [Fe] and pH, higher levels of degradation of the dye mixture are achieved for all the λ studied. Figure 4 shows that in case of the λ related to the aromatic groupings (234 and 258 nm), higher values of degradation are obtained for the lower pH level and a higher time of exposure to radiation, considering the difficulty involved in degrading these compounds. With regard to the chromophoric groups (λ of 428 and 482 nm), the same occurs when the lowest pH level is combined with any level of time. In Fig. 5 a and b, higher percentages of degradation are obtained for the λ of 428 and 482 nm by using lower pH and [Fe] levels, independently of the [H_2O_2] level. Figure 5c, for the same λ, shows that higher degradation values are obtained for the lower level of [Fe], independently of the time of radiation exposure.

The subsequent experiments were, therefore, performed using a pH of 3.5, [Fe] equal to 1.0 mg L^{-1}, and 50 mg L^{-1} of [H_2O_2]. The lowest [H_2O_2] was chosen in order to use this reagent without excess and to reduce costs, since higher degradations were obtained independently of the level of this parameter and the excess of this

Table 2 Effect estimates obtained using two-way ANOVA analysis for degradation of dye mixture

Factor	Wavelength (nm)									
	234		258		314		428		482	
	Effect ± error	*p**	Effect ± error	*p**	Effect ± error	*p**	Effect ± error	*p**	Effect ± error	*p**
X_1	− 4.60 ± 0.49	0.0109	− 2.10 ± 0.25	0.0141	3.27 ± 0.67	0.0389	0.94 ± 0.13	0.0004	2.61 ± 0.05	0.0175
X_1X_1	− 26.46 ± 1.22	0.0021	− 30.56 ± 0.63	0.0004	− 1.90 ± 1.67	**0.3728**	1.10 ± 0.32	0.0137	− 1.06 ± 0,12	**0.0743**
X_2	− 38.55 ± 0.49	0.0002	− 38.57 ± 0.25	0.0001	− 65.20 ± 0.67	0.0001	− 7.91 ± 0.13	0.0001	− 11.64 ± 0.05	0.0002
X_3	− 5.85 ± 0.49	0.0068	− 19.07 ± 0.25	0.0002	− 8.32 ± 0.67	0.0063	− 9.39 ± 0.13	0.0001	− 14.51 ± 0.05	0.0002
X_4	14.45 ± 0.49	0.0011	11.00 ± 0.25	0.0005	3.17 ± 0.67	0.0413	− 1.74 ± 0.13	0.0010	− 1.56 ± 0.05	0.0052
X_1X_2	− 0.22 ± 0.49	**0.6887**	− 0.35 ± 0.25	**0.2988**	− 1.27 ± 0.67	**0.1956**	1.31 ± 0.13	0.0007	1.84 ± 0.05	0.0091
X_1X_3	0.08 ± 0.49	**0.8914**	1.65 ± 0.25	**0.2250**	1.02 ± 0.67	**0.2636**	1.44 ± 0.13	0.0007	1.91 ± 0.05	0.0076
X_1X_4	0.57 ± 0,49	**0.3580**	0.72 ± 0.25	**0.1023**	0.22 ± 0.67	**0.7676**	1.24 ± 0.13	**0.3377**	0.06 ± 0.05	0.0102
X_2X_3	4.52 ± 0,49	0.0113	− 7.57 ± 0.25	0.0011	6.32 ± 0.67	0.0109	− 7.36 ± 0.13	0.0001	− 10.29 ± 0.05	0.0003
X_2X_4	− 1.62 ± 0,49	**0.0789**	0.30 ± 0.25	**0.3555**	− 1.17 ± 0.67	**0.2197**	− 0.91 ± 0.13	0.0045	− 0.74 ± 0.05	0.0185
X_3X_4	2.82 ± 0,49	0.0283	1.10 ± 0.25	0.0486	0.57 ± 0.67	**0.4788**	− 0.84 ± 0.13	0.0017	− 1.21 ± 0.05	0.0218
R^2	0.9926		0.9955		0.9949		0.9781		0.9889	
MS pure error	0.9433		0.2533		1.7733		0.0633		0.0110	

MS, mean squares; R^2, coefficient of determination

*The results of *p* values that are not significant with a confidence level of 95% are highlighted in bold type

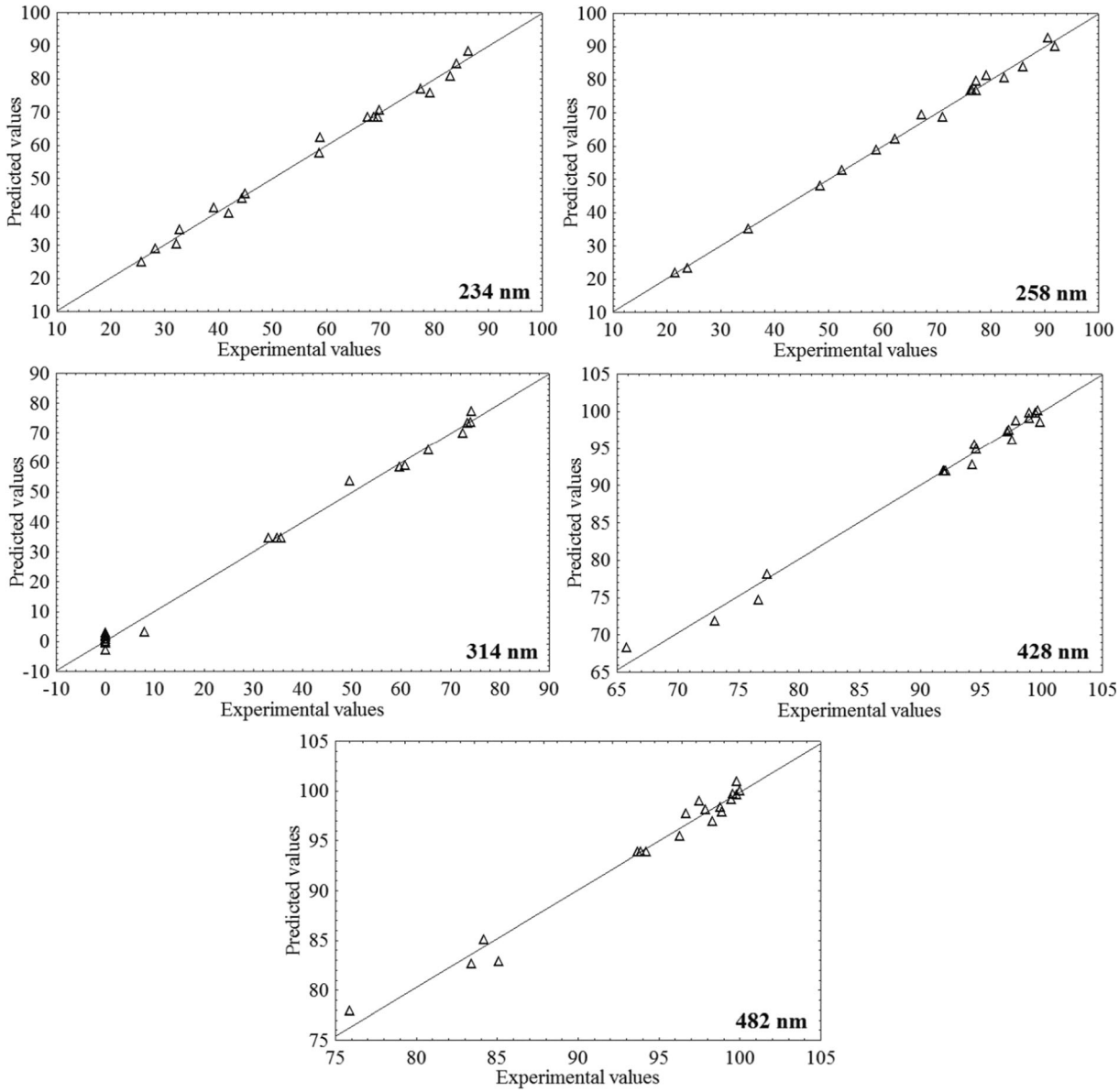

Fig. 2 Comparison of the percentages of experimental and predicted degradation obtained by the models

reagent acts by sequestering hydroxyl radicals, thus disfavoring the reaction.

Similar results were found by Santana et al. (2018) and Nascimento et al. (2018b), who studied the degradation of direct orange textile dye 26 and the mixture of remazol gold-yellow dyes RNL-150% and turquoise reactive Q-G125, respectively, using the photo-Fenton process.

2.4 Influence of Surface Area/Volume Ratio of the Solution on Degradation Efficiency

In this study, the efficiency of the photo-Fenton/UV-C system was evaluated as regards the degradation of the mixture of the SY and T dyes as a function of the A_{sup}/V_{sol} ratio. The results are shown in Fig. 6.

In Fig. 6, note that there is no significant difference in the degradation for the A_{sup}/V_{sol} relations studied for the λ of 428 and 482 nm. As the A_{sup}/V_{sol} ratio increases, a

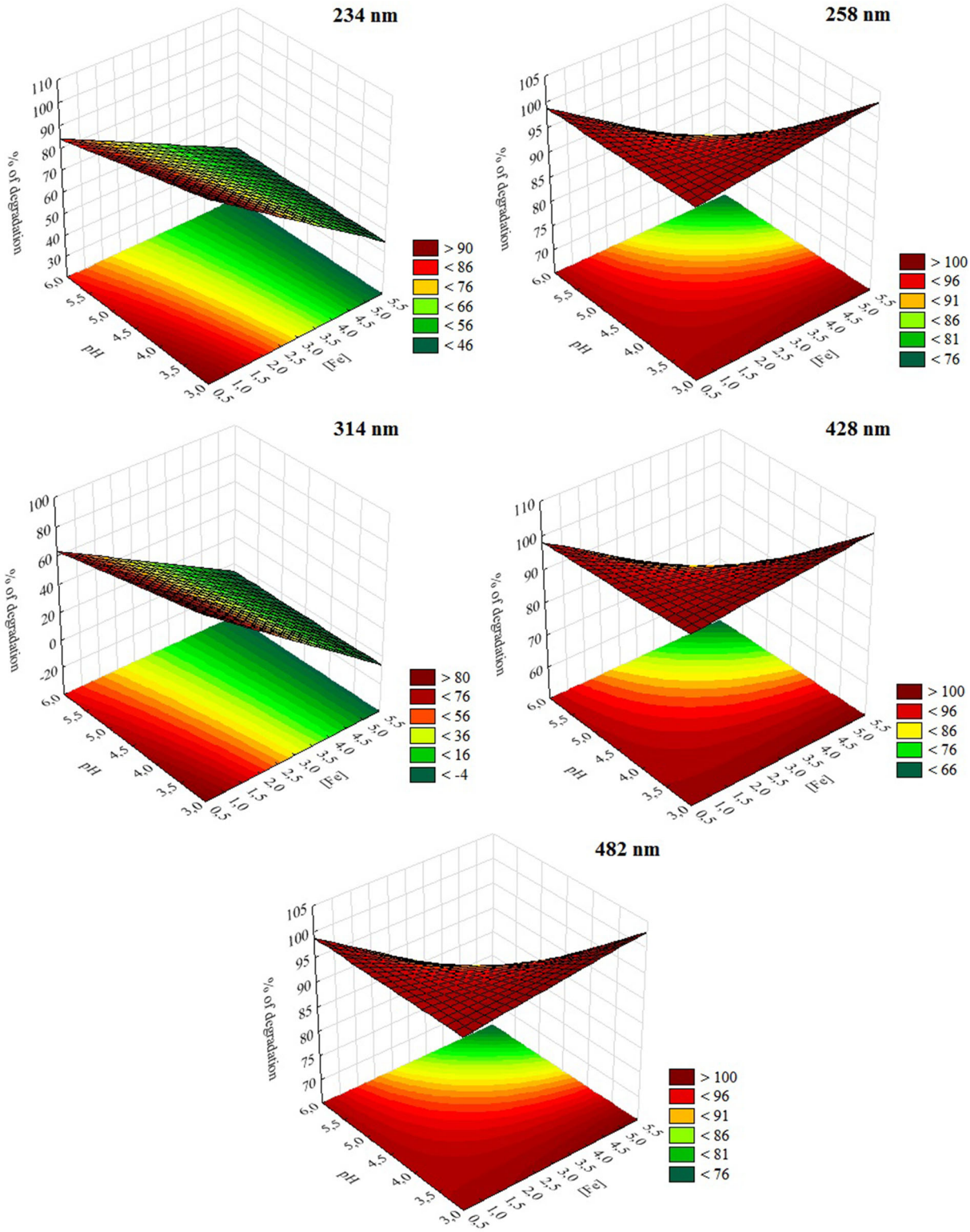

Fig. 3 Response surfaces for the % of degradation related to the of the interaction effect [Fe] (X_2) vs pH (X_3)

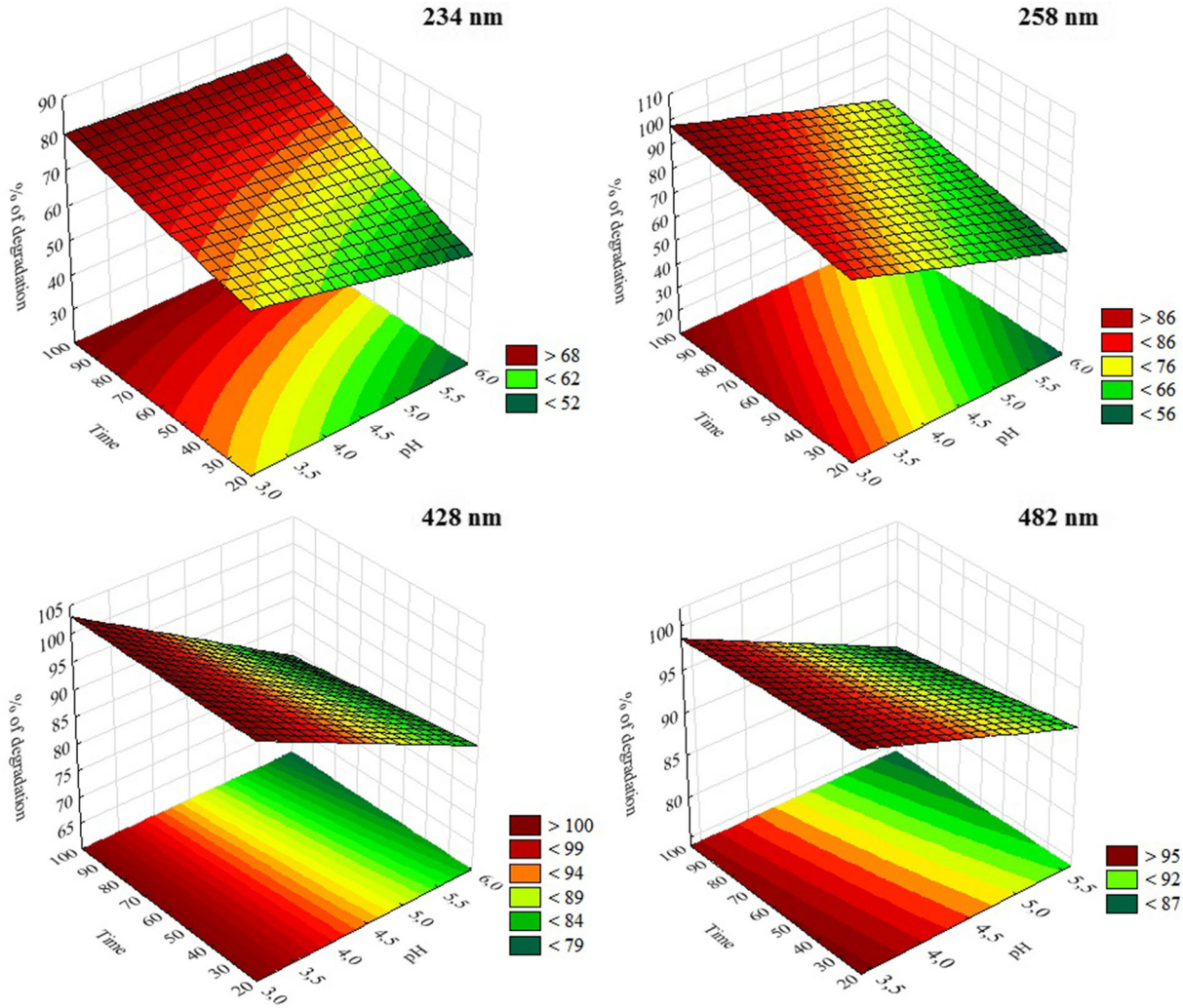

Fig. 4 Response surfaces for the % of degradation related to the of the interaction effect pH (X_3) vs time (X_4)

decrease in the percentages of degradation occurs for λ of 234, 258, and 314 nm. This indicates that the larger the volume of the solution to be treated and the greater the surface area of contact with the radiation, the greater the degradation efficiency in the relationships evaluated. The kinetic study was, therefore, performed using the A_{sup}/V_{sol} ratio of 0.02 cm^2 mL^{-1} (19.5 cm^2/1000 mL), with the objective of obtaining higher percentages of degradation of aromatic compounds (λ of 234, 258, and 314 nm).

2.5 Kinetic Evaluation of the Degradation of the Dye Mixture

The kinetic study of degradation was performed under the best conditions found in previous studies. The kinetic evolution of the degradation of the mixture of the SY and T dyes over time (C/C_0 vs t), along with the adjustment to the kinetic model proposed by Chan and Chu, residual values of the percentage of degradation over time, and spectral scans in the range of λ from 190 to 600 nm are presented in Fig. 7.

Stabilization of the system occurred after 50 min (Fig. 7a). At this time, the degradation was greater than 98% for λ at 482 and 428 nm, 93% at 258 nm, 87% at 234 nm, and 72% at 314 nm. It was also found that the experimental

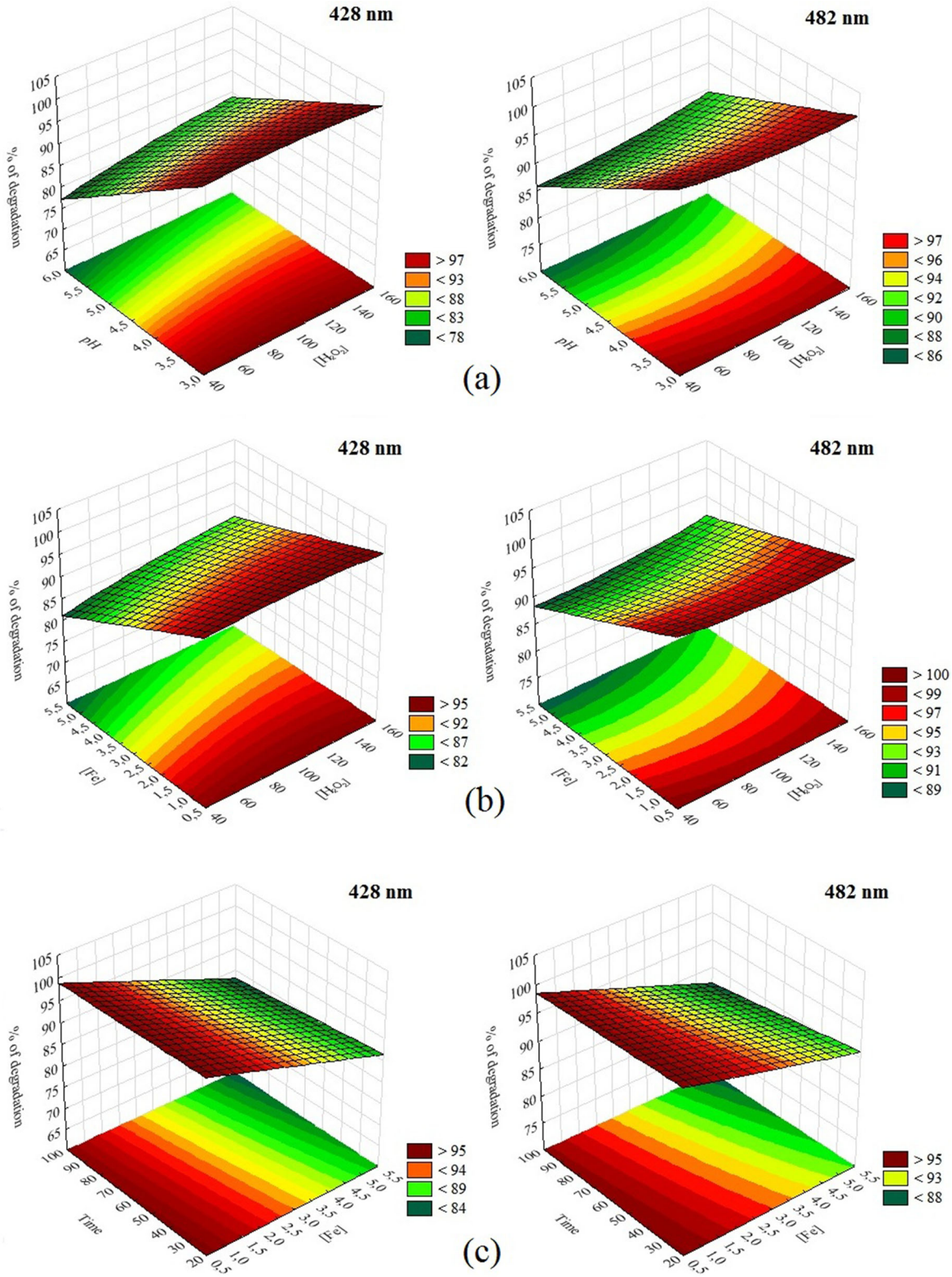

Fig. 5 Response surfaces for the % of degradation related to the of the interaction effects. **a** $[H_2O_2]$ (X_1) vs pH (X_3). **b** $[H_2O_2]$ (X_1) vs [Fe] (X_2). **c** [Fe] (X_2) vs time (X_4)

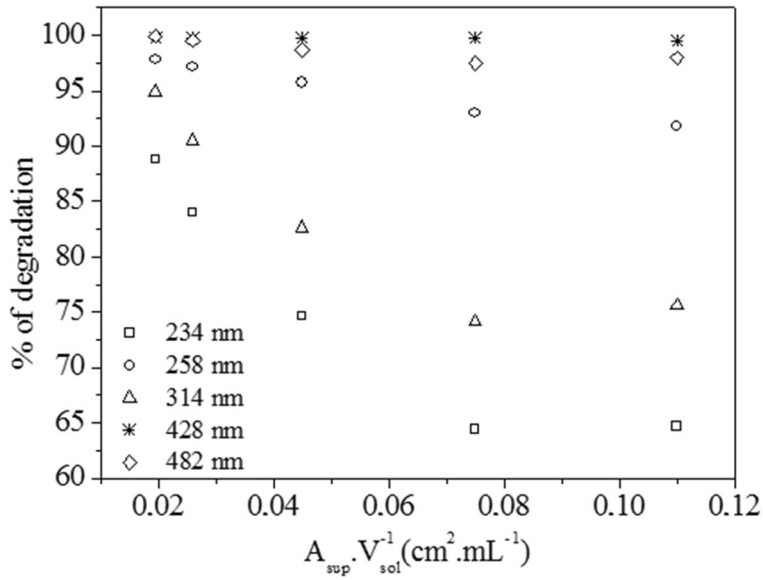

Fig. 6 Results of degradation of the dye mixture as a function of A_{sup}/V_{sol} ratio

data concerning the degradation of the dye mixture using the photo-Fenton process with UV-C radiation fitted well with the kinetic model proposed by Chan and Chu (2003). This good fit was confirmed by the behavior of the residuals left by the model (Fig. 7b), in which the data were randomly distributed and close to zero.

An analysis of Fig. 7c indicates that the photo-Fenton process using UV-C radiation was efficient as regards the degradation of λ of 234, 258, 428, and 482 nm, since the characteristic peaks of these λ were not visualized. This behavior indicated the possible effective destruction of the chromophore and the probable breakage of the aromatic rings of the dye molecules. With regard to the λ of 314 nm, the peak decreased gradually over time, but at a slower rate than the peaks of the other wavelengths. It is possible that the formation of intermediates did not occur, considering that new peaks were not observed.

In this context, it possible to affirm that the results obtained are promising, since literature shows that, in order to degrade food colors, it is often necessary to use heterogeneous photocatalysis, which may increase the cost of the process. Palas et al. (2017) used a perovskite $LaCuO_3$ (0.25 g L^{-1}) as a catalyst to degrade the tartrazine dye, obtaining 46.6 and 64.4% for the λ of 257 and 428 nm in 120 min of exposure to UV radiation. Rajamanickam and Shanthi (2014) evaluated the use of TiO_2 supported on activated carbon as a photocatalyst (1 g L^{-1}) in the degradation of the sunset yellow dye, obtaining 45.7% for the λ of 313 nm after 60 min of exposure to UV-A radiation.

The conversion data obtained after 180 min and the kinetic parameters of the oxidation reaction obtained from Eqs. (1) and 2 are shown in Table 3.

The linear regression coefficients (R^2) were higher than 0.95 and the ERRSQ values were low, indicating a good fit to the proposed model (Table 3). The initial removal rate ($1/\rho$) was higher for the λ of 428 and 482 nm, and a faster rate of reduction was attained for the chromophoric groups. In the case of the aromatic groups (λ of 234, 258, and 314 nm), the decrease ratio was slower owing to the difficulty involved in degrading these compounds. The maximum oxidation capacity of the system ($1/\sigma$) was similar for all the λ studied.

A quantification of the residual concentration of H_2O_2 was performed with the 180-min time sample from the kinetic study. The result found was in the range of 2 to 5 mg L^{-1}, showing that hydrogen peroxide was not fully consumed during the reaction.

2.6 Toxicity Study and Evaluation of Biodegradability

The treatment efficiency was evaluated by studying the toxicity of the samples before and after submission to the AOP under the same treatment conditions described for the 180-min time kinetic study using *Lactuca sativa* seeds. This was done by counting the number of seeds that germinated and their root growth. The relative growth index (RGI) and germination index (GI) were

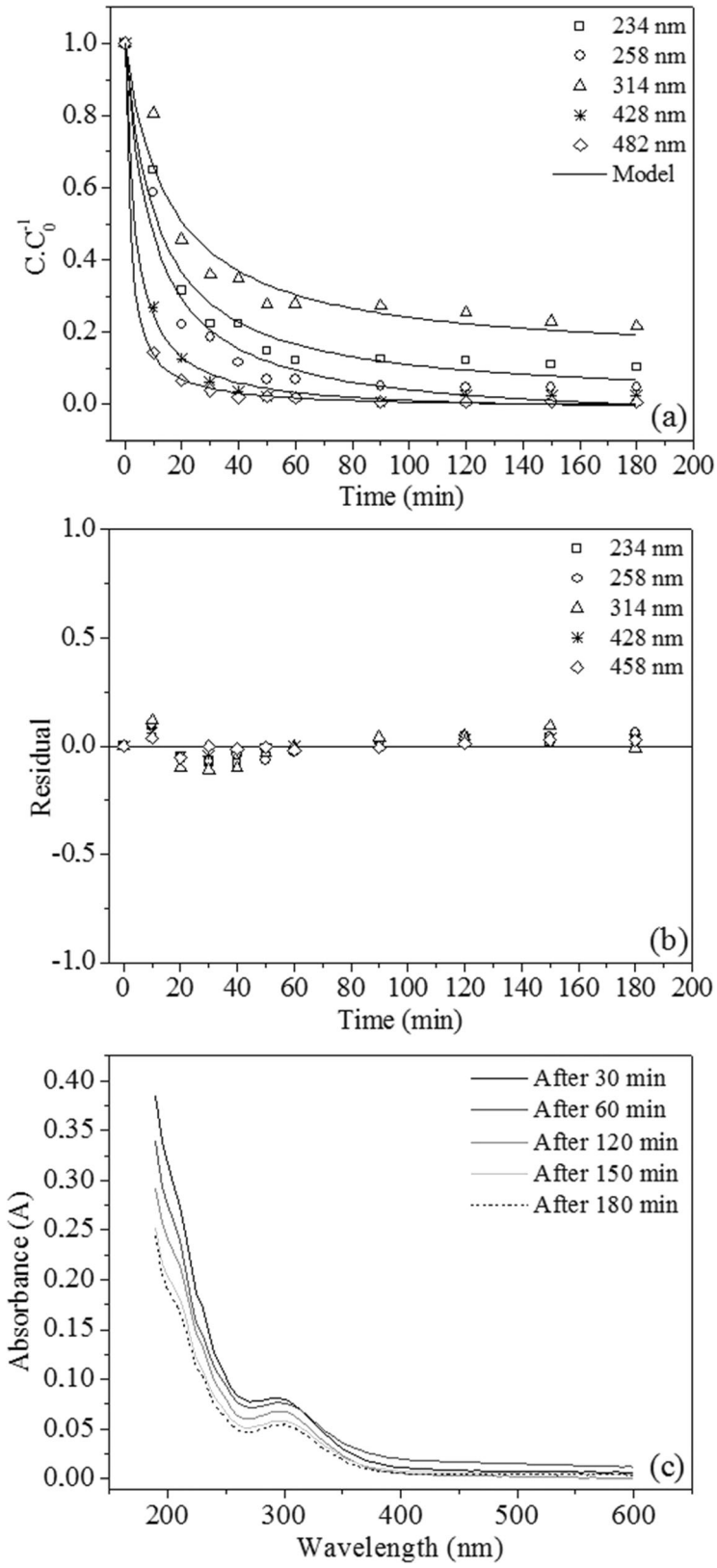

Fig. 7 Kinetic evaluation. **a** Adjustment to the kinetic model. **b** Residual of the percentage of degradation. **c** Absorption spectra of dye mixture after treatment

Table 3 Conversion and kinetic parameters calculated by the model

λ (nm)	X (%)	$1/\rho$	$1/\sigma$	R^2	ERRSQ
234	87.9	0.13	0.96	0.95	0.04
258	93.5	0.20	0.97	0.95	0.04
314	78.5	0.03	0.99	0.90	0.15
428	99.6	1.03	0.99	0.98	0.01
482	99.2	1.88	0.97	0.99	0.007

also calculated for a better analysis and understanding of the results (Table 4).

After analyzing Table 4, it was observed that the solutions of the SY and T dye mixture after the treatment with dilutions of 5 and 1% led to germination similar to that of the negative control. Germination similar to the sample before treatment was observed for the other dilutions, with GI values higher than the sample before treatment, thus indicating no increase in the toxicity of the samples after treatment.

The RGI results were higher than 0.80, indicating that there was, according to Young et al. (2012), no inhibition of growth. Santos et al. (2018) evaluated the toxicity of erythrosine and a bright blue dye mixture before and after the AOP, using *Lactuca sativa* seeds, and verified a reduction in the toxicity of the solution after treatment using the UV/H_2O_2/TiO_2 process.

The results of the mean and standard deviation (σ) of the bacterial activity of the samples for OD_{600} between the initial time and after 24 h of incubation are presented in Table 5, in addition to the cellular viability evaluation data obtained after 48 h of incubation.

The results of Table 5 show that, based on OD_{600} values, the bacterial growth of strains of *Escherichia coli* and *Salmonella enteritidis* had values higher than the negative control for solutions before and after treatment without dilution. The dilutions of these solutions, which had lower values than the negative control, were within the experimental error. The solutions studied were not, therefore, toxic for the bacterial species *Escherichia coli* and *Salmonella enteritidis*. The viability test showed that all the samples remained viable for the two bacterial species. Charamba et al. (2018) found that, after the use of the UV/H_2O_2 process for the degradation of leaf green and açaí purple dyes, there was a decrease in the toxicity of the dye solution for the strains of *Staphylococcus aureus* and *Staphylococcus pyogenes* bacteria.

Table 5 Bacterial toxicity results

Samples	*Escherichia coli*		*Salmonella enteritidis*	
	Mean ± σ (OD_{600})	Viability	Mean ± σ (OD_{600})	Viability
Negative control	0.321 ± 0.071	+++	0.345 ± 0.010	+++
SBT[a]	0.361 ± 0.013	+++	0.358 ± 0.009	+++
SBT 1:100	0.329 ± 0.003	+++	0.341 ± 0.001	+++
SBT 1:1000	0.293 ± 0.006	+++	0.314 ± 0.018	+++
SPT[b]	0.341 ± 0.001	+++	0.385 ± 0.015	+++
SPT 1:100	0.270 ± 0.010	+++	0.353 ± 0.012	+++
SPT 1:1000	0.296 ± 0.006	+++	0.319 ± 0.013	+++

[a] Solution before treatment; [b] Solution post-treatment

The results obtained in order to evaluate biodegradability (COD/BOD ratio) before and after the photo-Fenton process at 180 min were 34.28 and 4.39, respectively. The reduction in this ratio indicates that the treatment used was efficient as regards the degradation

Table 4 Results of *Lactuca sativa* toxicity test

Sample	Average number of seeds that germinated	Root growth, mean ± σ (cm)	RGI	GI (%)
Negative control	9.7 ± 0.6	8.7 ± 1.0	1.00	100.00
SBT[a]	7.7 ± 0.6	7.0 ± 0.1	0.88	69.55
SPT[b] 1%	9.3 ± 0.6	8.7 ± 0.2	1.00	96.55
SPT 5%	9.0 ± 1.0	8.5 ± 0.5	0.98	87.93
SPT 10%	8.7 ± 0.6	8.1 ± 0.1	0.93	87.02
SPT 50%	8.0 ± 1.0	7.6 ± 0.5	0.85	80.38
SPT 70%	8.0 ± 1.0	7.3 ± 0.6	0.81	76.84
SPT 100%	7.7 ± 0.6	7.0 ± 0.1	0.80	70.19

[a] Solution before treatment; [b] Solution post-treatment

of the mixture of SY and T dyes, resulting in an increase in the biodegradable fraction. Similar results were also found by Santos et al. 2018, who studied the photocatalytic degradation of a mixture containing erythrosine and bright blue food dyes.

3 Conclusions

The 2^4 factorial central composite design was successfully applied in order to establish the optimum conditions for the degradation of a sunset yellow and tartrazine dye mixture using the photo-Fenton/UV-C system. An analysis of variance (ANOVA) indicated that a second-order regression model fitted the experimental data well. Degradation percentages of over 99% were obtained for the chromophoric groups and were higher than 78% for the aromatic groups, in 180 min. The kinetic model proposed by Chan and Chu had a good fit to the experimental data. In the toxicity tests, no inhibition in growth was observed for the *Lactuca sativa* seeds and for the *Escherichia coli* and *Salmonella enteritidis* bacteria. The reduction in the COD/BOD ratio indicated an increase in the biodegradable fraction. It is, therefore, possible to conclude that the photo-Fenton/UV-C system can be used as an efficient treatment for the degradation of the mixture of the sunset yellow and tartrazine dyes.

Acknowledgments The authors are very grateful to the following Brazilian fostering agencies and institutions: Fundação de Amparo a Ciência e Tecnologia de Pernambuco (FACEPE), Fundação de Apoio ao Desenvolvimento da Universidade Federal de Pernambuco (FADE/UFPE), Núcleo de Química Analítica Avançada do Estado de Pernambuco (NUQAAPE/FACEPE), Coordenação de Aperfeiçoamento de Pessoal de Nível Superior (CAPES), and the Laboratory of Protein Biochemistry of UFPE.

Compliance with Ethical Standards

Conflict of Interest The authors declare that they have no conflict of interest.

References

Almeida, E. J. R., Andrade, A. R., & Corso, C. R. (2019). Evaluation of the acid blue 161 dye degradation through electrochemical oxidation combined with microbiological systems. *International journal of Environmental Science and Technology, 16*, 8185–8196. https://doi.org/10.1007/s13762-019-02377-5.

Banaschik, R., Jablonowskia, H., Bednarskic, P. J., & Kolb, J. F. (2018). Degradation and intermediates of diclofenac as instructive example for decomposition of recalcitrant pharmaceuticals by hydroxyl radicals generated with pulsed corona plasma in water. *Journal of Hazardous Materials, 342*, 651–660. https://doi.org/10.1016/j.jhazmat.2017.08.058.

Basu, A., & Kumar, G. S. (2015). Interaction of toxic azo dyes with heme protein: biophysical insights into the binding aspect of the food additive amaranth with human hemoglobin. *Journal of Hazardous Materials, 289*, 204–209. https://doi.org/10.1016/j.jhazmat.2015.02.044.

Carocho, M., Barreiro, M. F., Morales, P., & Ferreira, I. C. F. R. (2014). Adding molecules to food, pros and cons: a review on synthetic and natural food additives. *Comprehensive Reviews in Food Science and Food Safety, 13*, 377–399. https://doi.org/10.1111/1541-4337.12065.

Cetinkaya, S. G., Morcali, M. H., Akarsu, S., Ziba, C. A., & Dolaz, M. (2018). Comparison of classic Fenton with ultrasound Fenton processes on industrial textile wastewater. *Sustainable Environment Research, 28*, 165–170. https://doi.org/10.1016/j.serj.2018.02.001.

Chan, K. H., & Chu, W. (2003). Modeling the reaction kinetics of Fenton's process on the removal of atrazine. *Chemosphere, 51*, 305–311. https://doi.org/10.1016/S0045-6535(02)00812-3.

Charamba, L. V. C., da Rocha Santana, R. M., do Nascimento, G. E., Charamba, B. V. C., de Moura, M. C., Coelho, L. C. B. B., de Oliveira, J. G. C., Duarte, M. M. M. B., Napoleão, D. C., & (2018). Application of the advanced oxidative process on the degradation of the green leaf and purple açaí food dyes with kinetic monitoring and artificial neural network modelling. *Water Science and Technology, 78*(5), 1094–1103.

Chekira, N., Tassalit, D., Benhabiles, O., Merzouk, N. K., Ghenna, M., Abdessemed, A., & Issaadi, R. (2017). A comparative study of tartrazine degradation using UV and solar fixed bed reactors. *International Journal of Hydrogen Energy, 42*, 8948–8954. https://doi.org/10.1016/j.ijhydene.2016.11.057.

Chung, K. T. (2016). Azo dyes and human health: a review. *Journal of Environmental Science and Health, Part C, 34*, 233–261. https://doi.org/10.1080/10590501.2016.1236602.

Elbanna, K., Sarhan, O. M., Khider, M., Elmogy, M., Abulreesh, H. H., & Shaaban, M. R. (2017). Microbiological, histological, and biochemical evidence for the adverse effects of food azo dyes on rats. *Journal of Food and Drug Analysis, 25*, 667–680. https://doi.org/10.1016/j.jfda.2017.01.005.

Gadekar, M. R., & Ahammed, M. M. (2019). Modelling dye removal by adsorption onto water treatment residuals using combined response surface methodology-artificial neural network approach. *Journal of Environmental Management, 231*, 241–248. https://doi.org/10.1016/j.jenvman.2018.10.017.

Ghoneim, M. M., El-Desoky, H. S., & Zidan, N. M. (2011). Electro-Fenton oxidation of sunset yellow FCF azo-dye in aqueous solutions. *Desalination, 274*, 22–30. https://doi.org/10.1016/j.desal.2011.01.062.

Gupta, V. K., Jain, R., Nayak, A., Agarwal, S., & Shrivastava, M. (2011). Removal of the hazardous dye - tartrazine by photodegradation on titanium dioxide surface. *Materials*

Science and Engineering C, 31, 1062–1067. https://doi.org/10.1016/j.msec.2011.03.006.

Khayyat, L., Essawy, A., Sorour, J., & Soffar, A. (2017). Tartrazine induces structural and functional aberrations and genotoxic effects in vivo. *Journal of Life and Environmental Sciences, 5*, e3041. https://doi.org/10.7717/peerj.3041.

Lipskikh, O. I., Korotkova, E. I., Khristunova, Y. E. P., Barek, J., & Kratochvil, B. (2018). Sensors for voltammetric determination of food azo dyes - a critical review. *Electrochimica Acta, 260*, 974–985. https://doi.org/10.1016/j.electacta.2017.12.027.

Montgomery, D. C. (2008). *Design and analysis of experiments*. EUA: Wiley.

Nagel-Hassemer, M. E., Carvalho-Pinto, C. R. S., Matias, W. G., & Lapolli, F. R. (2011). Removal of coloured compounds from textile industry effluents by UV/H_2O_2 advanced oxidation and toxicity evaluation. *Environmental Technology, 32*, 1867–1874. https://doi.org/10.1080/09593330.2011.566893.

Nair, A. T., Makwana, A. R., & Ahammed, M. M. (2014). The use of response surface methodology for modelling and analysis of water and wastewater treatment processes: a review. *Water Science and Technology, 69*, 464–478. https://doi.org/10.2166/wst.2013.733.

Nascimento, G. E., Napoleão, D. C., Silva, P. K. A., Santana, R. M. R., Bastos, A. M. R., Zaidan, L. E. M. C., Moura, M. C., Coelho, L. C. B. B., & Duarte, M. M. M. B. (2018a). Photo-assisted degradation, toxicological assessment, and modeling using artificial neural networks of reactive gray BF-2R dye. *Water, Air, & Soil Pollution, 229*, 1–15. https://doi.org/10.1007/s11270-018-4028-2.

Nascimento, G. E., Napoleão, D. C., Santana, R. M. R., Charamba, L. V. C., Oliveira, J. G. C., Moura, M. C., Coelho, L. C. B. B., & Duarte, M. M. M. B. (2018b). Degradation of textile dyes remazol yellow gold and reactive turquoise: optimization, toxicity and modeling by artificial neural networks. *Water Science and Technology, 2017*, 812–823. https://doi.org/10.2166/wst.2018.251.

Oancea, P., & Meltzer, V. (2013). Photo-Fenton process for the degradation of tartrazine (E102) in aqueous medium. *Journal of the Taiwan Institute of Chemical Engineers, 44*, 990–994. https://doi.org/10.1016/j.jtice.2013.03.014.

Okafor, S. N., Obonga, W., Ezeokonkwo, M. A., Nurudeen, J., Orovwigho, U., & Ahiabuike, J. (2016). Assessment of the health implications of synthetic and natural food colourants - a critical review. *UK Journal of Pharmaceutical and Biosciences, 4*, 1–11. https://doi.org/10.20510/ukjpb/4/i4/110639.

Oller, I., Malato, S., & Sánchez-Pérez, J. A. (2011). Combination of advanced oxidation processes and biological treatments for wastewater decontamination – a review. *Science of the Total Environment, 409*, 4141–4166. https://doi.org/10.1016/j.scitotenv.2010.08.061.

Palas, B., Ersöz, G., & Atalay, S. (2017). Photo Fenton-like oxidation of tartrazine under visible and UV light irradiation in the presence of $LaCuO_3$ perovskite catalyst. *Process Safety and Environmental Protection, 111*, 270–282. https://doi.org/10.1016/j.psep.2017.07.022.

Peláez-Cid, A.-A., Herrera-González, A.-M., Salazar-Villanueva, M., & Bautista-Hernández, A. (2016). Elimination of textile dyes using activated carbons prepared from vegetable residues and their characterization. *Journal of Environmental Management, 181*, 269–278. https://doi.org/10.1016/j.jenvman.2016.06.026.

Rajamanickam, D., & Shanthi, M. (2014). Photocatalytic degradation of an azo dye sunset yellow under UV-A light using TiO_2/CAC composite catalysts. *Spectrochimica Acta, Part A: Molecular and Biomolecular Spectroscopy, 128*, 100–108. https://doi.org/10.1016/j.saa.2014.02.126.

Rice, E. W., Baird, R. B., Eaton, A. D., & Clesceri, L. S. (2012). *Standard methods for the examination of water and wastewater*. Washington: American Public Health Association.

Rizzo, L. (2011). Bioassays as a tool for evaluating advanced oxidation processes in water and wastewater treatment. *Water Research, 45*, 4311–4340. https://doi.org/10.1016/j.watres.2011.05.035.

Rovina, K., Prabakaran, P. P., Siddiquee, S., & Shaarani, S. M. (2016). Methods for the analysis of sunset yellow FCF (E110) in food and beverage products- a review. *Trends in Analytical Chemistry, 85*, 47–56. https://doi.org/10.1016/j.trac.2016.05.009.

Santana, R. M. R., Nascimento, G. E., Silva, P. K. A., Lucena, A. L. A., Procópio, T. F., Napoleão, T. H., Duarte, M. M. M. B., & Napoleão, D. C. (2018). Kinetic and ecotoxicological evaluation of the direct orange 26 dye degradation by Fenton and solar photo-Fenton processes. *Revista Eletrônica em Gestão, Educação e Tecnologia Ambiental, 22*, 1–20. https://doi.org/10.5902/2236117032254.

Santiago, D. E., González-Díaz, O., Araña, J., Melián, E. P., Pérez-Peña, J., & Doña-Rodríguez, J. M. (2018). Factorial experimental design of imazalil-containing wastewater to be treated by Fenton-based processes. *Journal of Photochemistry and Photobiology A: Chemistry, 353*, 240–250. https://doi.org/10.1016/j.jphotochem.2017.11.038.

Santos, M. M. M., Duarte, M. M. M. B., Nascimento, G. E., Souza, N. B. G., & Rocha, O. R. S. (2018). Use of TiO_2 photocatalyst supported on residues of polystyrene packaging and its applicability on the removal of food dyes. *Environmental Technology, 12*, 1–14. https://doi.org/10.1080/09593330.2017.1423396.

Shojaeimehr, T., Rahimpour, F., Khadivi, M. A., & Sadeghi, M. (2014). A modeling study by response surface methodology (RSM) and artificial neural network (ANN) on Cu^{2+} adsorption optimization using light expended clay aggregate (LECA). *Journal of Industrial and Engineering Chemistry, 20*, 870–880. https://doi.org/10.1016/j.jiec.2013.06.017.

Soares, B. M., Araujo, T. M., Ramos, J. A., Pinto, L. C., Khayat, B. M., De Oliveira Bahia, M., & Khayat, A. S. (2015). Effects on DNA repair in human lymphocytes exposed to the food dye tartrazine yellow. *Anticancer Research, 35*, 1465–1474.

Tikhomirova, T. I., Ramazanova, G. R., & Apyari, V. V. (2018). Effect of nature and structure of synthetic anionic food dyes on their sorption onto different sorbents: peculiarities and prospects. *Microchemical Journal, 143*, 305–311. https://doi.org/10.1016/j.microc.2018.08.022.

Vedrenne, M., Vasquez-Medrano, R., Prato-Garcia, D., Frontana-Uribe, B. A., Hernandez-Esparza, M., & Andrés, J. M. (2012). A ferrous oxalate mediated photo-Fenton system: toward an increased biodegradability of indigo dyed wastewaters. *Journal of Hazardous Materials, 243*, 292–301. https://doi.org/10.1016/j.jhazmat.2012.10.032.

Wang, J. L., & Xu, L. J. (2012). Advanced oxidation processes for wastewater treatment: formation of hydroxyl radical and application. *Critical Reviews in Environmental Science and Technology, 42*, 251–325. https://doi.org/10.1080/10643389.2010.507698.

Wang, Y., Zhuang, Z., Xiao, Y., & Li, N. (2014). Spectrophotometric determination of sunset yellow in beverage after preconcentration by the cloud point extraction method. *Analytical Methods, 6*, 8901–8905. https://doi.org/10.1039/C4AY01537A.

Young, B. J., Riera, N. I., Beily, M. E., Bres, P. A., Crespo, D. C., & Ronco, A. E. (2012). Toxicity of the effluent from an anaerobic bioreactor treating cereal residues on *Lactuca sativa*. *Ecotoxicology and Environmental Safety, 76*, 182–186. https://doi.org/10.1016/j.ecoenv.2011.09.019.

Zaidan, L. E. M. C., Rodriguez-Díaz, J. M., Napoleão, D. C., Montenegro, M. C. B. S. M., Araújo, A. N., Benachour, M., & Silva, V. L. (2017). Heterogeneous photocatalytic degradation of phenol and derivatives by ($BiPO_4/H_2O_2$/UV and TiO_2/H_2O_2/UV) and the evaluation of plant seed toxicity tests. *Korean Journal of Chemical Engineering, 34*, 511–522. https://doi.org/10.1007/s11814-016-0293-1.